

## ON THE DEVELOPMENT OF DOPPLER GLOBAL VELOCIMETRY FOR CRYOGENIC WIND TUNNELS

C. Willert, G. Stockhausen, J. Klinner, M. Beversdorff  
Institute of Propulsion Technology, German Aerospace Center (DLR)  
Linder Höhe, 51147 Köln, Germany

J. Quest, U. Jansen  
European Transonic Windtunnel (ETW)  
Ernst-Mach-Straße, 51147 Köln, Germany

M. Raffel  
Institute of Aerodynamics and Flow Technology, German Aerospace Center (DLR)  
Bunsenstraße 10, 37073 Göttingen, Germany

### **ABSTRACT**

A specially designed Doppler global velocimetry system (DGV, planar Doppler velocimetry) was tested in a high-speed cryogenic facility at Mach 0.3 to Mach 0.8 and pressures between 1.2 and 2.5 bar. The necessary seeding was achieved by injecting a mixture of gaseous nitrogen and water vapor into the dry and cold tunnel flow which then immediately formed a large amount of small ice crystals. As operational and access conditions are quite restrictive with respect to other facilities, DGV is currently considered the best choice for the non-intrusive measurement of flow fields. A comparison of DGV to the more wide-spread particle image velocimetry technique (PIV) is also given.

### **INTRODUCTION**

Cryogenic wind tunnels are of special interest in aerodynamic research because they permit the increase of model Reynolds number by drastically lowering the gas temperature. Due to the variation of the gas temperature, the influence of Mach number and Reynolds number on the aerodynamic coefficients of model measurements can be investigated separately. This in turn allows for more realistic comparisons to full scale aircraft.

The cryogenic environment with temperatures as low as 100K, however, imposes severe requirements on both model design and any sort of instrumentation such that mainly conventional techniques have been used, for example: force balances, surface pressure scanners, Pitot rakes, five-hole probes, and the like. More recently surface techniques such as Moiré interferometry<sup>1</sup>, temperature/pressure sensitive paint<sup>2</sup> or infrared imaging techniques, were qualified. Laser-based flow velocimetry such as particle image velocimetry (PIV) or velocimetry based on Doppler shift measurements (DGV, LDV) thus far were considered too complex and costly for use in cryogenic facilities although they already have reached a high level of maturity in standard- as well as large scale industrial wind tunnels. As most common laser velocimetry techniques rely on the

presence of light scatters (seeding material) one of the principal issues that had to be resolved was that of adequately seeding the dry cryogenic flow. With seeding in place, a number of other issues such as laser light sheet generation, optical access, calibration, etc., had to be solved. The following article gives an overview of the specific measures necessary to install the DGV system and presents some results from a first test campaign.

In this context it should be noted that the PIV technique recently was successfully applied in the cryogenic wind tunnel Cologne (DNW-KKK), a low-speed facility with a closed tunnel circuit.<sup>3</sup> Experiences collected in this context allow for a performance comparison between the two techniques.

### **CRYOGENIC WIND TUNNEL FACILITY**

The European Transonic Wind tunnel (ETW) is a closed-circuit facility with a 2.4 x 2 m<sup>2</sup> test section that can reach a free stream Mach number of 1.3 at temperatures down to 110K and pressures up to 4.5 bar (Fig. 1). Its primary use is the nearly realistic simulation of cruise flight conditions of modern aircraft. Cryogenic test conditions are established through the injection of liquid nitrogen (LN<sub>2</sub>) which lowers the tunnels gas temperature through its evaporation. As up to 50MW are required to drive the tunnel circuit, large amounts of liquid nitrogen – sometimes exceeding 100 kg per second – are needed to compensate for the generated heat and maintain the temperature set point. This makes facility operation very costly and therefore rapid data acquisition is a prerequisite for any diagnostic technique to be utilized – typical set-point hold times are on the order a few seconds only. As shown in Fig. 1 the test section itself is enclosed by a 10m diameter pressure vessel which is inaccessible during tunnel operations. Direct optical access to the test section from the outside is also not possible. This implies that any hardware installed in the tunnel pressure plenum has to withstand pressure changes, requires shielding for the cryogenic environment and

must be able operate autonomously or through remote control. As high power lasers (Class IV type) generally require water cooling and/or frequent manual fine tuning they must be located outside of the plenum with appropriate beam delivery to the measurement areas.

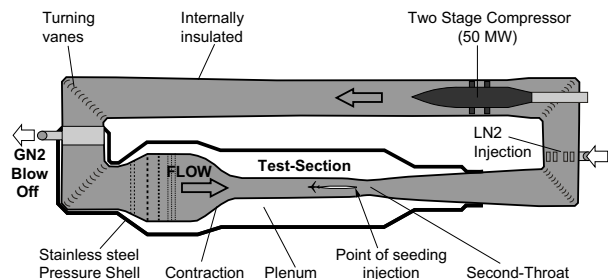


Fig. 1: Cross-section of the ETW cryogenic wind tunnel.

### SEEDING ISSUES

A number of seeding visibility tests were performed in recent years and involved imaging of a laser beam or light sheet with a video camera in both the DNW-KKK as well as ETW.<sup>4</sup> The results were generally inconclusive, that is, in some cases strong scattering signals with the presence of ice-clusters could be observed whereas in other cases the light beam was only very weakly visible. Residual humidity and the presence of traces of water or carbon dioxide in the liquid nitrogen were considered as possible causes of these irreproducible results. In either case, *natural* seeding was insufficient to reliably establish laser-based velocimetry in the cryogenic flow.

Consequently a series of further tests toward *active* seeding was conducted. These included introducing traces of carbon-dioxide or water as well as aerosols. For the application of PIV in the DNW-KKK facility an oil dispersing Laskin-nozzle seeding generator was supplied with dry nitrogen gas. This system produced droplets on the order of 1  $\mu\text{m}$  diameter. An arrangement of 40 impactor nozzles of 1.5 mm diameter each accelerated the particle-laden flow toward an impactor plate at 1.5 mm distance from the impactor nozzles. These impactors together with an additional settling vessel separated the larger droplets from the seeding prior to its injection into the tunnel. During the recent PIV measurement campaign at DNW-KKK, it has been estimated that less than 1 ml oil is required the tunnel during the test campaign. Based on the recorded PIV image data a seeding density of up to 10 particles/ $\text{mm}^3$  could be achieved during the experiments after continuously seeding the tunnel for 5 minutes (this corresponds to  $\approx 30$  particles per PIV interrogation volume).

Nevertheless this (frozen) oil droplet seeding is insufficient for reliable DGV measurements – typical camera exposure times of 2 to 5 seconds could only provide saturation levels of less than 5%. In other words, at least a 10-fold increase of seeding would be required which in turn increases the chance of tunnel contamination. The main reason for the increased seeding requirement stems from the fact that while

PIV images discrete particles with best possible fidelity (high contrast), DGV requires a homogenous distribution of scattered light. Therefore a well seeded PIV image has a mean intensity of 5–10% of the sensor's dynamic range.

An alternative and very efficient form of tracer generation can be achieved by injecting a stream of warm nitrogen and water vapor (e.g. from an industrial steam cleaning system) into the tunnel. Once this flow mixes with the dry, saturated cryogenic atmosphere it immediately forms tiny ice crystals (sublimation) without any liquid phase. In itself this is a very noteworthy and respectable action from the side of the tunnel operators as great measures are generally taken to keep tunnel humidity at a minimum during cool-down and operation. Once introduced into the flow this ice seeding was observed to persist up to 15 minutes in the closed circuit flow of the DNW-KKK (Figs. 2–4), whereas the continuous blow-off in the ETW results in a gradual decay in seeding luminosity over time. Little is currently known with regard to size of the ice crystals as PIV images were not recorded at the time of these tests. Finally one of the primary advantages of this seeding method is that it leaves no residue after the measurement. Seeding the ETW facility for DGV involved a continuous injection of about 1 kg/s dry nitrogen (dew point  $-80^\circ\text{C}$ ) mixed with saturated steam. The actual water concentration in the tunnel atmosphere was approximately 200ppm at  $\text{Ma}=0.3$  with  $T=190\text{K}$ ,  $P=125\text{kPa}$ .

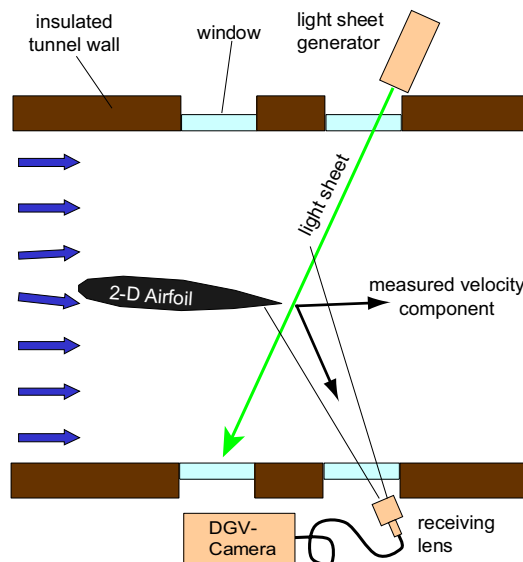


Fig.2: Imaging arrangement for seeding tests at DNW-KKK.

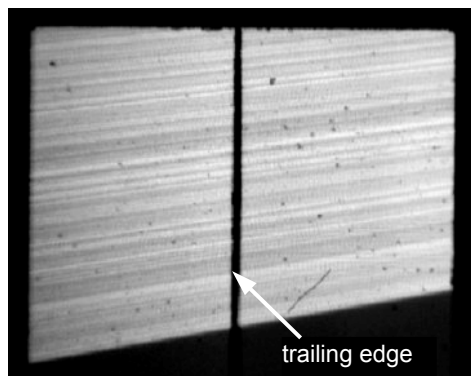


Fig. 3: Image of light sheet of seeded flow as viewed by DGV camera using a (flexible) imaging fiber bundle. Tunnel conditions: T=130K, U≈30 m/s.. Stripes are due to irregularities on tunnel windows. Black spots are imperfections in imaging bundle (broken fibers).

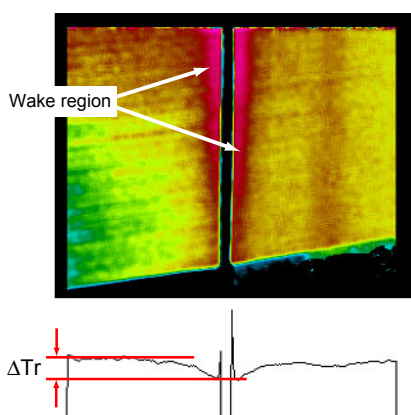


Fig. 4: Qualitative DGV transmission image of airfoil wake flow (laser system was not calibrated). The transmission difference of  $\Delta Tr \approx 8\%$  corresponds to velocity difference of  $\approx 20$  m/s.

### DGV SUBSYSTEM

Doppler Global Velocimetry (DGV) is a technique which provides planar velocity data through the imaging of light-sheet illuminated particles suspended in the flow. Contrary to PIV, which infers the flow's velocity by measuring the displacement of particle images over a given time interval, DGV relies on the indirect measurement of the frequency shift of light scattered by the particles. This is achieved by carefully tuning the laser onto a transitional slope of an molecular absorption band (typically iodine vapor) such that a frequency shift results in a change of light transmission through the molecular absorber. In practice an iodine vapor cell of constant vapor pressure, placed in front of a CCD camera, is used as the frequency-to-intensity converter. A second (reference) camera placed in front of the iodine cell is used for the normalization of the generally non-uniform light intensity of the imaged light sheet. The measured Doppler shift  $\Delta f$  is directly related to the combination incident light direction  $\vec{o}$  and observation direction  $\vec{l}$  through the relation:

$$\Delta f \lambda_{\text{Laser}} = (\vec{o} - \vec{l}) \cdot \vec{U}$$

Therefore a single camera imaging a single light sheet can only provide a single velocity component. Measurements of all three velocity components therefore require a combination of multiple viewing positions or multiple (coplanar) light sheet directions.

Whereas it is possible in principle to perform DGV measurements of unsteady flow similar to PIV, the approach followed at DLR was to optimize the method for the measurement of *time-averaged* velocity data. While this might seem like a limitation on first thought, it brings along a number technological and practical simplifications and advantages. For instance continuous-wave (CW) lasers may be used which may be transmitted through flexible fibers and generally are much simpler to frequency-stabilize than pulsed versions. Further, a single camera that images multiple light sheets of different incidence is much more cost effective than a multiple-camera setup which would be required for pulsed DGV. Finally issues arising through the statistically varying, time-dependent speckle nature of laser light are effectively integrated out when averaging the received light over time.

Installation of a DGV system inside the ETW facility required the solution of several, previously untackled problems. For one, the tunnel test section remains inaccessible during any measurement campaign such that all equipment has to be remotely controlled. Also, there is no direct optical access to the tunnel test section from outside the enclosing pressure plenum. To add to the complexity, equipment placed inside the pressure plenum must be able to withstand both elevated pressures and cryogenic temperatures and/or have be appropriately shielded from this environment.

Due to limited optical access and space constraints in the ETW facility the classical *triple-light-sheet-single-camera* configuration described previously was considered unfeasible. The high thermal and aerodynamic loading at high Mach numbers makes an imaging arrangement as described for the PIV measurements impossible here. Instead multiple cameras placed behind windows on the side walls of the test section obliquely view two coplanar light sheets spanning the test section (Figs. 6,7). This viewing arrangement has the advantage that no equipment disturbs the high-speed cryogenic flow (not even the tunnel boundary layer) with the added benefit of using the generally much stronger (~10-fold) forward-scatter light signal. One drawback of this configuration is that Doppler shift decreases with increased forward scattering angle. A number of additional hardware-specific aspects of this DGV system are described next.

### DGV Camera system

While the triple-viewing arrangement would normally require three separate DGV camera systems (e.g. six CCD cameras and three iodine cells), a novel approach was chosen using a *multiple branch imaging fiber bundle*.<sup>5</sup> On the entry side of each branch a standard CCD-format objective lenses

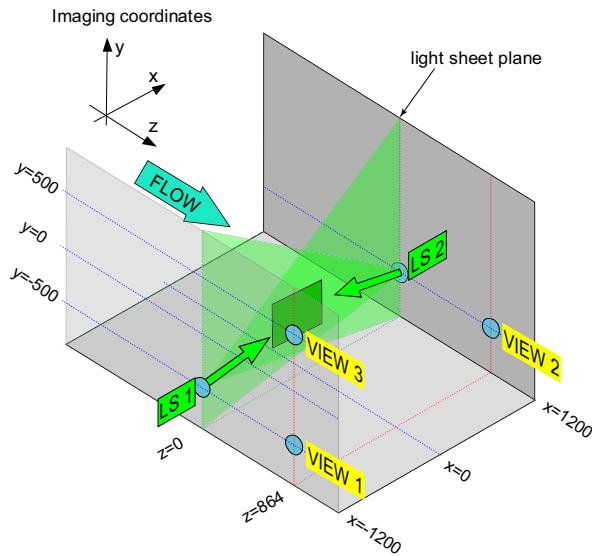


Fig. 6: DGV imaging arrangement in the ETW wind tunnel.

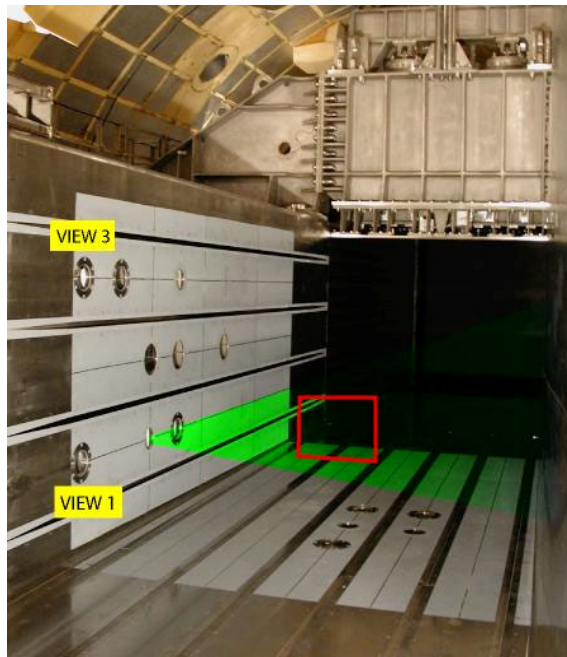


Fig. 7: Photograph of the 2.4 m wide ETW test section with top wall removed. The red rectangle gives the approximate position of the imaged area.

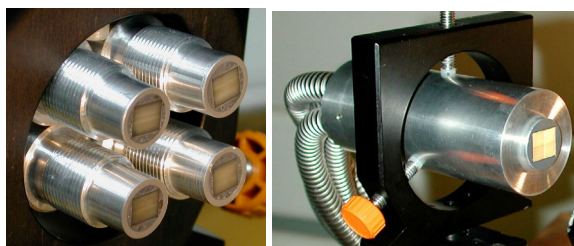


Fig. 8: Left: Entry faces of the multiple branch fiber imaging bundle without imaging lenses. Each branch is 4.5m long and consists of 500 x 400 individual fibers with a pitch of 10  $\mu\text{m}$ . Right: combined exit face of the 4 branches.

images the collected light onto the fiber bundle which then transmits the image along 4.5m to the remotely located DGV camera system. On the exit side four individual bundles are merged into a common end consisting of four quadrants (see Fig. 8)

Figure 9 shows the actual DGV camera system which has been optimized for high light efficiency. A high aperture photographic macro-lens ( $f=85\text{mm}$ ,  $f\# 1.8$ ) in reverse imaging direction collects much of the light emitted by the high aperture ( $N.A. \approx 0.60$ ) of the imaging fiber bundle. The light leaving the lens is nearly collimated before entering the beam splitter followed by the iodine vapor absorption cell. This collimated beam of light is then imaged onto the two CCD sensors (1380 x 1040 pixel spatial resolution at 12 bits/pixel) using a pair of large aperture photographic lenses ( $f=50\text{mm}$ ,  $f\# 1.4$ ).

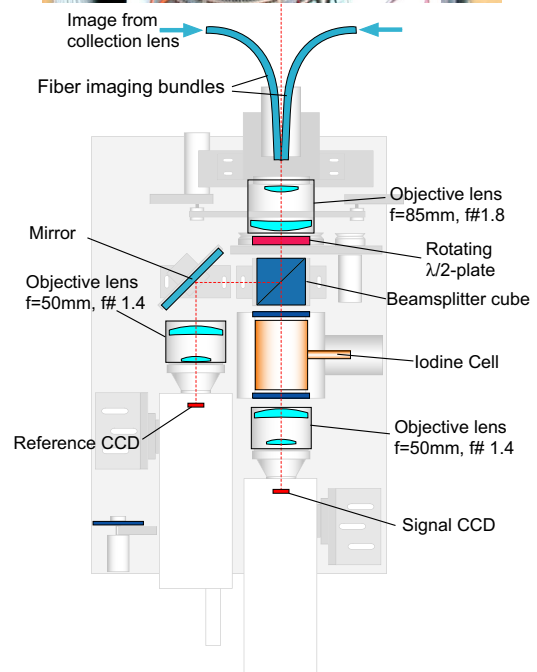


Fig. 9: DGV camera system mounted inside a thermally insulated box below the test section

Performance-wise the spatial resolution was sufficient to nearly resolve the 10  $\mu\text{m}$  fiber pitch of the imaging bundle while vignette resulted in a intensity drop-off down to 50 percent on the edges. The overall aperture of the system was estimated to be around  $f\# 2$ , yielding about twice the light sensitivity of systems described in the past.<sup>6,7</sup> The splitting ratio of the non-polarizing, laser-line beam splitting cube was chosen at 30%R / 70%T to account for nearly 50% of non-resonant light absorption through the iodine cell and thereby ensured similar illumination levels of the CCD sensors. Since even non-polarizing beam splitters were found to exhibit a significant angle-dependent residual sensitivity to polarization, a half-wave plate rotating at  $\approx 2\text{Hz}$  was placed in front of the beam splitter cube with the aim of depolarizing the collected light over time. Finally, a remote-controlled focussing system on the first objective lens was intended for focus-adjustment during pressure-induced index of refraction changes.

The entire camera system was packaged inside a thermally insulated, heated enclosure which was mounted below the test section at a position from which the three branches of the imaging fiber bundle could reach the three different viewing positions on opposite sides of the tunnel. The images recorded by the CCD cameras were transmitted to the host computer system via fiber-optic (network-grade) duplex cables.

The remaining, fourth branch of the image bundle system was used to monitor the laser frequency and intensity. The transmission signal obtained from this quadrant directly provided the averaged (!) laser frequency for the duration of the camera exposure and thereby improves the system measurement accuracy. This approach is also very efficient because in the past this signal was generally obtained through additional (lengthy) measurement procedures.

**DGV Light Sheet Generation**

The time-averaging nature of the DGV implementation described herein makes it possible to use a sweeping beam for the generation of the light sheet which is not possible with the pulsed light of Nd:YAG PIV lasers. Figure 10 outlines the optical arrangement of the scanning beam light sheet generator that is supplied with laser light through a multi-mode fiber of 15 m length and a core diameter of 10  $\mu\text{m}$ . The dynamic element in this optical system is a rotating glass octagon that periodically displaces a nearly parallel beam. A cylindrical lens

then converts this displacement into an angular deflection thereby creating a light sheet. Additional plano-convex lenses determine the focal point within the light sheet. An octagon was chosen in place of a square because the light intensity drop-off toward the edges increases from 45% to 85%.

For calibration purposes a remote-controlled solenoid flips a grid into the optical path to generate a striped light sheet. A photodiode allows a remote optimization of the fiber delivery.

**DGV Data Processing**

The first step in the analysis of the recorded image data is to obtain the image projection coefficients that map the three obliquely viewed camera scenes onto a common (cartesian) grid. This is achieved by processing images of a common grid (dot pattern) placed into the light sheet plane prior to the measurement. By additionally displacing the grid in a known out-of-plane direction, the camera (viewing) coordinates can be estimated further easing the geometric calibration process.

Images of the fiber bundle are characterized by a significant degree of high-frequency modulation which in part is due to manufacturing defects and variations as well as due to the high resolving power of the DGV camera system. If not treated properly, these intensity modulations result in strong signal amplitudes in the ratio images (transmission images) – for this reason low-pass filtering is applied to the image data (9 x 9 Gaussian on 690 x 520 pixel images).

The actual iodine cell transmission images are obtained by normalizing the low-pass filtered image with similar images obtained at a non-Doppler shift sensitive laser frequency. A frequency lookup table is then used to back out the actual frequency shifts from the cell transmission. Given three of these frequency shift images (one for each camera view), the imaging geometry together with the light sheet directions is then used to finally obtain the velocity map.

**DGV Results**

In the process of establishing the DGV technique in the ETW facility for use in mapping the flow downstream of different wing tip devices (M-DAW EC-project) a preliminary test campaign provided insight into the system’s overall performance. The measurement campaign involved running the facility at low Mach numbers ( $Ma=0.3$ ) to optimize and calibrate the DGV imaging equipment before obtaining data for the high-speed runs ( $Ma=0.8$ ).

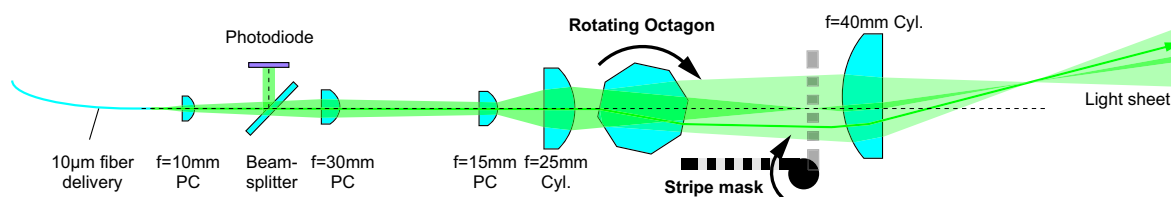


Fig. 10: Dynamic light sheet generator of DGV system.

With the water vapor seeding in place, camera exposures between 1 and 2 seconds were sufficient to reach 50% of sensor saturation. This meant that an image set comprised of one image pair for each of the two light sheets could be acquired within 5 seconds.

This *mock* campaign also proved very valuable in bringing out a number of previously unknown or underestimated problems and issues. One of the biggest problems arose due to background illumination: The tunnel test section walls are covered with diffuse gray paint which tends to scatter light in every direction. Laser light from the light sheet hitting the opposite wall therefore is scattered throughout the test section and illuminates the background viewed by the camera scenes. This light contamination can be handled by recording images without the presence of seeding. However, with seeding in place the background not only gains intensity (additional light scattering from particles), but the scattered light also has a frequency shift imposed on it depending on the flow velocity. This effect was so strong that the high-speed data was essentially rendered useless for quantitative analysis. As a consequence of this the tunnel background will be painted with dull black for the actual wing tip wake measurements.

Figure 11 shows the Doppler shift images obtained at  $Ma=0.3$  and clearly gives an impression of the irregular shape of the area viewed by each camera. Each image is characterized by a continuous gradient of frequency from left to right, which is due to the variation in viewing angle (the flow itself is nearly uniform). On the right edge, which coincides with the tunnel center line, two small structure are visible. These are due to a pair of vortex generators mounted on a rake approximately 0.40 m upstream of the light sheet. The wake of the rake is also faintly visible in views No.2 and No.3. The three views of Figure 11 are combined in the velocity map of Figure 12. While the measured mean velocity is quite plausible the data exhibits an unrealistic top-to-bottom velocity gradient – an effect most likely due to the background lighting of the camera views. The grainy structure on the images are due to the irregularities on the fiber imaging bundles and have amplitudes of 1–5 MHz. In the velocity maps this corresponds to fluctuations of 2–5 m/s.

Table 1 gives an impression of the measurement uncertainty achievable with the described system in comparison to a *classical* configuration using three light sheets and one camera. Especially the horizontal velocity component has a high measurement uncertainty, but it can be dramatically reduced when a backward scattering signal is available. Although backward scattering is roughly 10 times weaker than forward scattering and thus suffers a decrease in signal-to-noise ratio a weighted average of both forward and backward signal may improve the overall result. It is hoped that the additional treatment of the scene background

with flat black paint will make a capture of backward scattered signals possible.

## **CONCLUSIONS**

A large amount of information, some of it beyond the scope of this article, was gathered in the context of developing the Doppler global velocimetry technique for use in the ETW cryogenic wind tunnel. Although the data presented herein is only of preliminary nature with an *actual* measurement campaign to follow, the system's functionality nevertheless could be demonstrated.

Given the experiences gained from a recent PIV measurement campaign at DNW-KKK it is possible to compare the respective advantages and disadvantages of the two velocimetry technique which is summarized in Table 2. When considering the complexity of the DGV technique it is certainly advisable to use the simpler PIV technique whenever possible. The strengths of DGV on the other hand are its rapid data acquisition, its remote imaging and illumination capabilities as well as its flexibility with regard to the imaging configuration. For this reason DGV applications have been limited to applications where the PIV technique fails or is difficult to implement<sup>6,7,8</sup>.

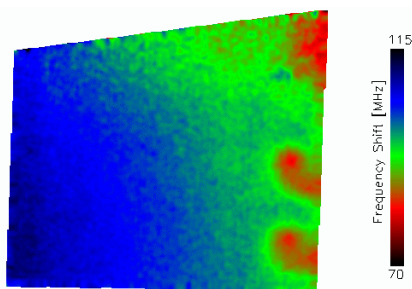
Currently, we consider DGV to be the only feasible technique for obtaining flow field data from the high-speed ETW facility. The future will certainly bring the technological advances allowing even pulsed PIV lasers to be installed in the pressure plenum of ETW. However, issues such as particle image blurring due to temperature gradients (wall boundary layer), type of seeding (diameter < 1 $\mu$ m) or strong vibrations also have to be addressed before stereoscopic PIV can be qualified.

## **ACKNOWLEDGMENTS**

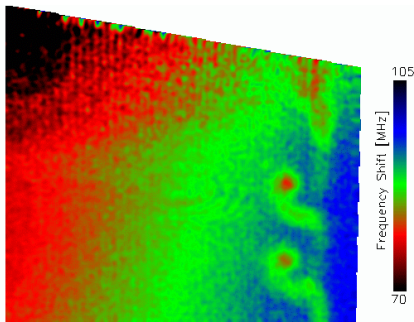
The activities described in this report are the result of a large number of different collaborators to whom the authors are very grateful. These include the ETW operation crew who were instrumental in the design, manufacture and installation of the measurement hardware. Special thanks go to Dr. Gerd Hefer for his courage of willingly contaminating the dry nitrogen tunnel atmosphere with water for the reliable generation of seeding which laid the foundation toward a successful application of DGV at ETW.

The M-DAW project ("Modelling and Design of Advanced Wing tip devices") is partly funded through the European Commission within the 5<sup>th</sup> Frame Work Programme and is coordinated by Airbus UK. DGV-measurement data yet to be obtained within this project will be processed by ONERA and then made available to the M-DAW consortium for comparison with numerical simulation.

View 1



View 2



View 3

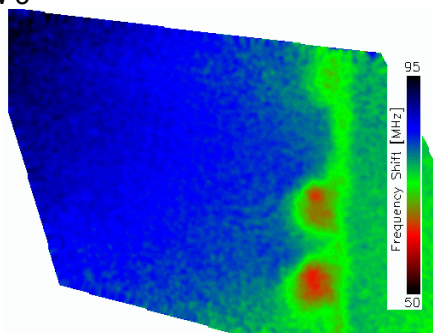


Fig. 10: Doppler-shift images obtained of the flow downstream of two vortex generators at  $Ma=0.3$ ,  $T=194$ ,  $P_{tot}=125kPa$

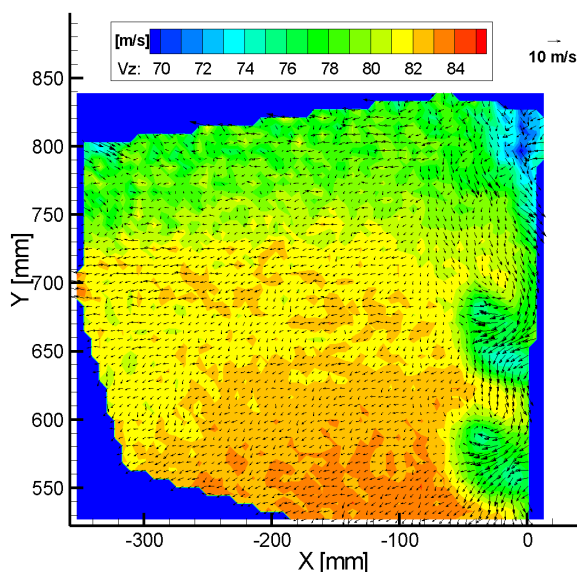


Fig. 11: Velocity map of the flow downstream of two vortex generators at  $Ma=0.3$ ,  $T=194$ ,  $P_{tot}=125kPa$ .

## REFERENCES

- 1.) Pallek D, Bütetfisch K A, Quest J, Strudthoff W, 2003, "Model Deformation Measurement in ETW using the Moire Technique", Proc.: *20th International Congress on Instrumentation in Aerospace Simulation Facilities (ICIASF)*, Göttingen, Germany, Aug. 25-29.
- 2.) Fey U, Engler R H, Egami Y, Iijima Y, Asai K, Jansen U, Quest J, 2003, "Transition Detection by Temperature Sensitive Paint at Cryogenic Temperatures in the European Transonic Wind Tunnel (ETW)", Proc.: *20th International Congress on Instrumentation in Aerospace Simulation Facilities (ICIASF)*, Göttingen, Germany, Aug. 25-29.
- 4.) Willert C, Bütetfisch K A, 1997, "Determination of cluster in the undisturbed flow of the ETW", DLR-Report: DLR-IB 223-97 C40.
- 3.) Richard H, Becker W, Loose S, Thimm M, Bosbach J, Raffel M, 2003, "Application of particle image velocimetry under cryogenic conditions", Proc.: *20th International Congress on Instrumentation in Aerospace Simulation Facilities (ICIASF)*, Göttingen, Germany, Aug. 25-29.
- 5.) Nobes D, Ford H, Tatam R, 2002, "Three component planar Doppler velocimetry using imaging fibre bundles", Proc. *11th Intl. Symp. on Applic. Laser Techniques to Fluid Mechanics*, Lisbon, Portugal, 8–11 July.
- 6.) Roehle I, Schodl R, Voigt P, Willert C, 2000, "Recent developments and applications of quantitative laser light sheet measuring techniques in turbomachinery components", *Measurement Science & Technology*, Vol. 11, pp. 1023-1035.
- 7.) Roehle I, Willert C, 2001, "Extension of Doppler global velocimetry to periodic flows", *Measurement Science & Technology*, Vol. 12, pp. 420-431.
- 8.) Willert C, Roehle I, Schodl R, Dingel O, Seidel T, 2002, "Application of planar doppler velocitmetry within piston engine cylinders", Proc. *11th Intl. Symp. on Applic. Laser Techniques to Fluid Mechanics*, Lisbon, Portugal, 8–11 July.

**Table 1:** DGV-measurement uncertainty based on a frequency uncertainty of  $\Delta f=1$  MHz which itself corresponds to a transmission uncertainty of 0.25%. (U,V are in-plane velocity, W the out-of-plane component)

Viewing arrangement	$\Delta U$ [m/s]	$\Delta V$ [m/s]	$\Delta W$ [m/s]
forward scattering	2.78	1.97	1.04
backward scattering	0.28	1.69	0.91
optimal <sup>fn</sup>	0.59	0.59	0.41

<sup>fn</sup>) optimal DGV viewing: light sheets arranged at 120° angles, orthogonal viewing

**Table 2:** Performance comparison between PIV and DGV application in cryogenic environment

<b>Particle Image Velocimetry</b>	<b>Doppler Global Velocimetry</b>
<ul style="list-style-type: none"> <li>• provides 2-C data, 3-C with increased complexity</li> <li>• unsteady measurement</li> <li>• lengthy averaging procedure, but have RMS-data (<math>\approx 1</math> minute for 100 recordings)</li> <li>• strong sensitivity to main flow vector (requires adjustment of <math>\tau</math> and light sheet thickness)</li> <li>• good performance in low to medium speed flows</li> <li>• requires good optical resolving power (=short depth of field) may suffer from temperature induced refraction changes</li> <li>• intrusive installation on sting or similar to get flow-normal velocity components (for 2-C config.)</li> <li>• requires direct light sheet delivery</li> <li>• low seeding concentration</li> <li>• requires <math>\geq 1 \mu\text{m}</math> particles from dedicated seeding generator (possible oil residue)</li> <li>• medium to low sensitivity to background light (can use high-pass filters)</li> <li>• most PIV hardware readily available</li> </ul>	<ul style="list-style-type: none"> <li>• provides 3-C velocity</li> <li>• no unsteady data</li> <li>• fast, time-averaged measurement (<math>&lt; 5</math> s per data set)</li> <li>• all velocity components with similar sensitivity</li> <li>• good performance in medium to high speed flows</li> <li>• optical distortion tolerable, imaging through flexible fiber bundles</li> <li>• non-intrusive installation behind tunnel walls</li> <li>• fiber-based laser light delivery</li> <li>• seeding concentrations <math>\approx 10</math>x higher</li> <li>• works with tiny ice-crystals, simple seeding method without residue (accumulation of ice possible)</li> <li>• strong sensitivity to background light / reflections (requires special treatment of background)</li> <li>• custom designed, complex hardware</li> </ul>